Supporting Information for

Structure Matters: Correlating Temperature Dependent Electrical Transport through Alkyl Monolayers with IR absorption and UV Photoelectron Spectroscopies.

Hagay Shpaisman[#], Oliver Seitz[%], Omer Yaffe[#], Katy Roodenko[%], Luc Scheres[$], Han Zuilhof[$], Yves J. Chabal[%], Tomoki Sueyoshi[&], Satoshi Kera[&], Nobuo Ueno[&], Ayelet Vilan[#] & David Cahen[#].

[#] *Dept. of Materials & Interfaces, Weizmann Inst. of Science, Rehovot 76100 Israel*

[%] *Dept. of Materials Science and Engineering, University of Texas at Dallas, Richardson, Texas 75080 USA*

[$] *Laboratory of Organic Chemistry, Wageningen University, Dreijenplein 8, Wageningen 6703 HB, the Netherlands*

[&] *Graduate School of Advanced Integration Science, Chiba University,*

Inage-ku, Chiba 263-8522, Japan

The first part of the supporting information consists of measurements on control samples (**Figures S1**) so as to assure that the effect of the current increase with decreasing temperature is a molecular feature.

The second part (**Figures S2-S3**) shows the stability and reproducibility of our electron transport measurements.

The third part (**Figure S4**) shows the I-V-T for n^{++}-Si-C18/Hg substrate, that were dominated by the temperature dependence of the Si space charge.

Finally, the fourth and last part includes additional information regarding the FTIR measurements (**Figure S5**) as well as an explanation as to how the calculations for the analysis of the IR spectra were performed (**pages 5-10**).

Suppprting Information for SC-EDG-09-2011-000639

Figure S1 shows I-V-T plots for the case where instead of molecules we have a Silicon Oxide layer. Figure S1 clearly shows that with an oxide layer a positive temperature effect is observed as expected for a hopping mechan-

ism.
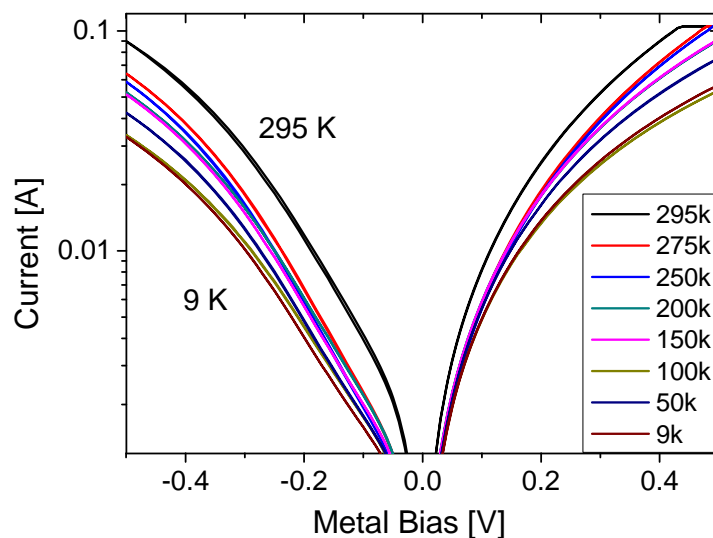
Figure S1: I-V-T curves for p^{++}-Si- SiO_x/Hg junctions. The temperature was varied between 9 K and 295 K. Currents decrease with decreasing temperature as expected for a hopping mechanism.

To understand if there is any contribution from the liquid solid transition (melting point 234K) we plot in **Figure S2** the current at 0.2 V (bias on the metal) as a function of temperature. As no abrupt change is observed we conclude that the liquid to solid transition did not change the contact area or influence the measure-

ment.
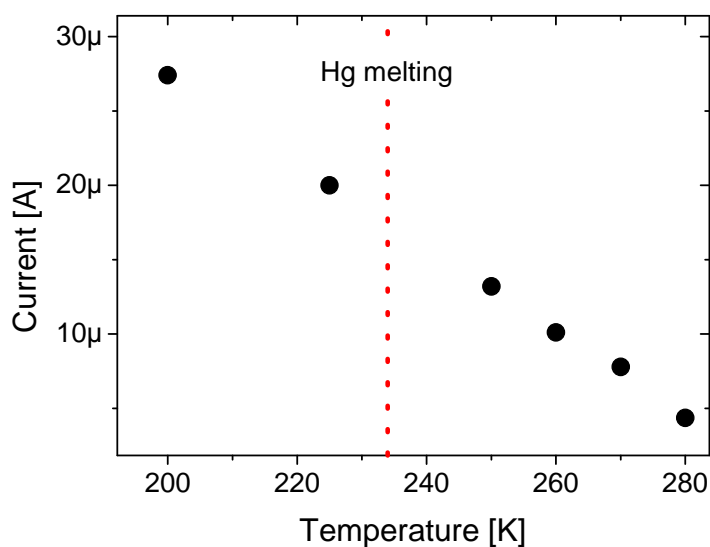
Figure S2: Zoom-in of the current as a function of temperature near the Hg melting temperature (234 K) for a C18 monolayer at a metal bias of 0.2 V. No abrupt changes

are seen around the melting temperature of Hg.

Figure S3 illustrates the reproducibility of our electron transport measurements. As controlling the exact size of the mercury droplet is extremely difficult with our current equipment, we show reproducibility for multiple measurements on the same droplet.
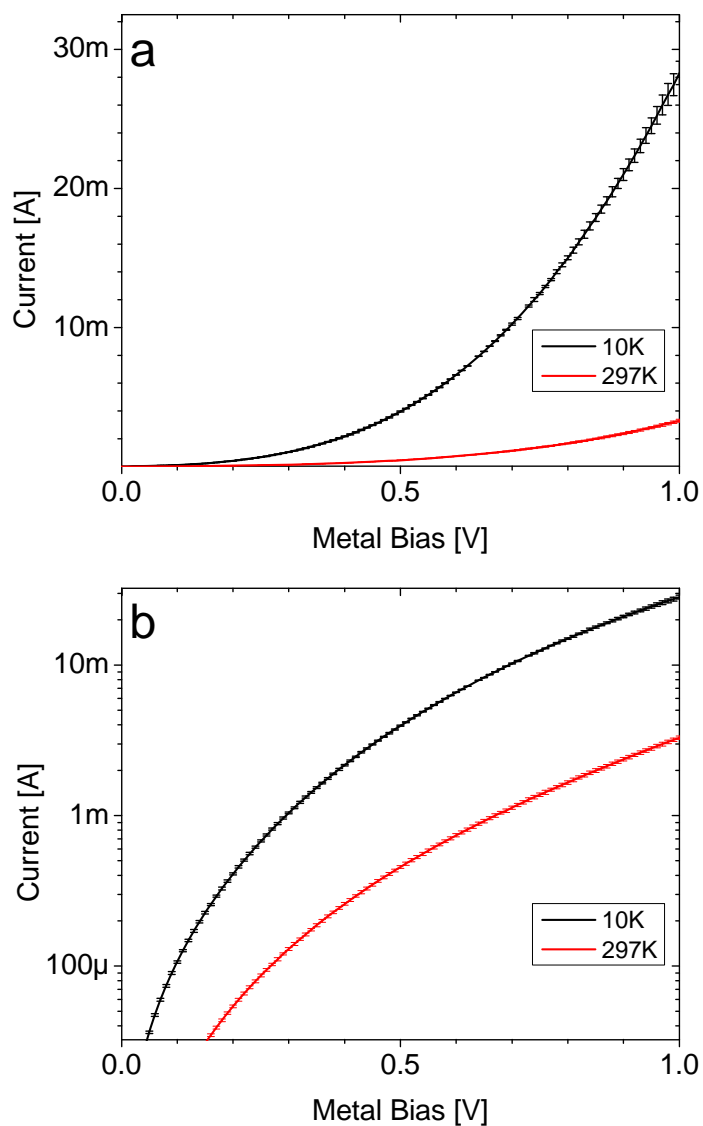
Figure S3: *Error bars for Currents as function of Voltage, calculated from six re-peating I-V-T measurements for a* Si-$(CH_2)_{17}$-CH_3 *(C18) monolayer (same sample with same Hg drop) at 297 K and 10 K, on a linear (a) and semi-log (b) current scales.*

Suppprting Information for SC-EDG-09-2011-000639

Figure S4 brings for comparison the I-V-T of highly doped n-Si. It shows that the molecular effect basically exists also for this type of doping though it is severely truncated by the opposite temperature effect on the space-charge of the Si. The much larger space charge in n^{++}-Si-alkyl/Hg compared to p^{++}-Si-alkyl/Hg is elaborated in ref. 37 and is clear from the ~ 3 orders of magnitude reduction in net current for n^{++} junctions compared to p^{++} ones (compare Fig. S4a to Fig. 1a of main text).
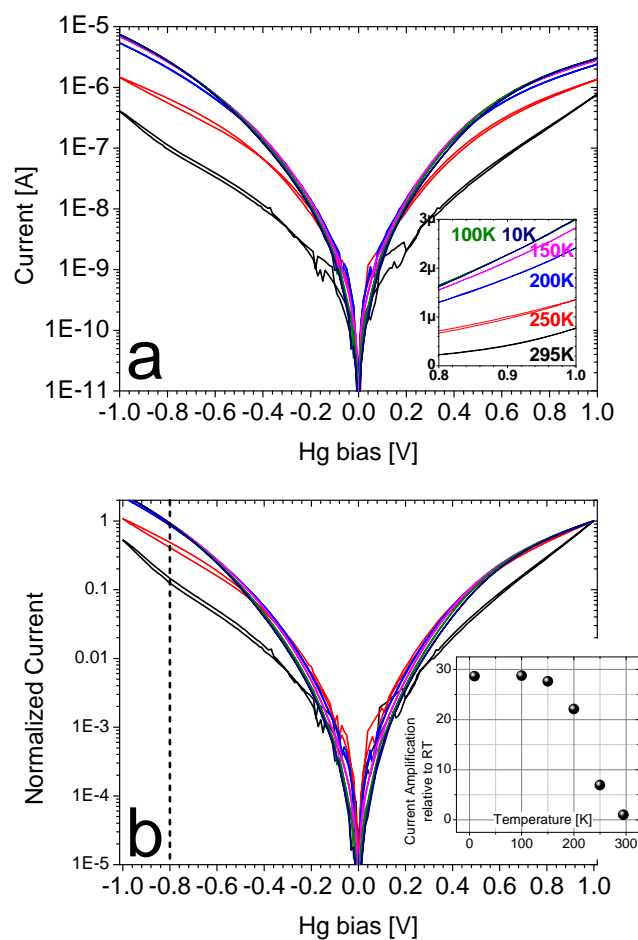
Figure S4: *Temperature-dependent current-voltage data for a n^{++}-Si-(CH$_2$)$_{17}$-CH$_3$ (C18) monolayer with a Hg top contact. a) raw data. b) same data normalized by dividing by the current at +1 V. Inset to (a) magnifies on a linear scale the high positive bias range and labels the different temperatures. Inset to (b) shows the current amplification at each temperature with respect to room temperature. Amplification was computed at V=-0.8V, where the amplification was maximal. The net amplification of ~ 30 folds is similar to that reported in main text for p^{++} junctions.*

Suppprting Information for SC-EDG-09-2011-000639
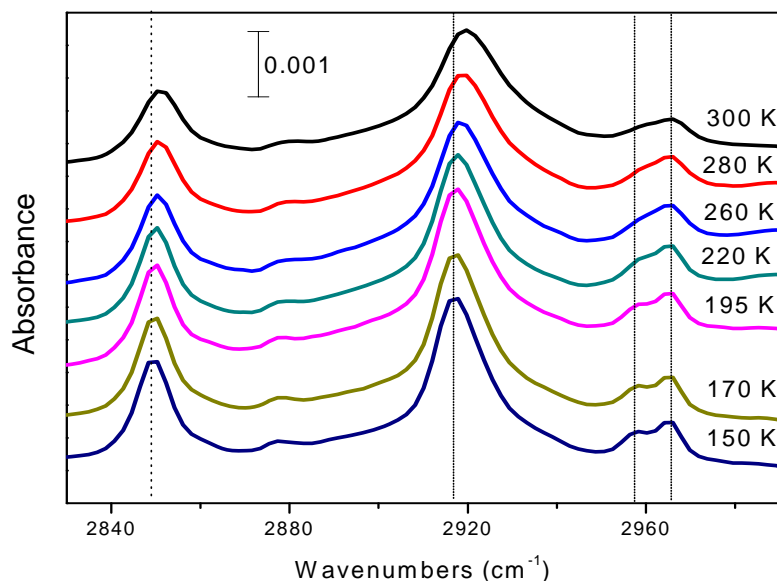
Figure S5: *IR spectra, as a function of temperature, in the 2800-3000 cm^{-1} region, where the fingerprint of the long hydrocarbon chains is pronounced. The bands at 2919 and 2851 cm^{-1} are assigned to the asymmetric $v_{as}(CH_2)$ and symmetric $v_s(CH_2)$ methylene stretch modes, respectively. The two peaks at 2959 and 2965 cm^{-1}, and the band at 2878 cm^{-1} are assigned to the two asymmetric $v_{as}(CH_3)$ and the symmetric $v_s(CH_3)$ methyl stretch modes, respectively. As the temperature decreases from 300 K to 150 K, the asymmetric $v_{as}(CH_2)$ and symmetric $v_s(CH_2)$ methylene stretch bands are red-shifted from 2919 and 2851 cm^{-1} to 2917 and 2849 cm^{-1}, respectively. Furthermore the two asymmetric $v_{as}(CH_3)$ modes become more distinct from each other.*

Calculations of the tilt angle from polarized FTIR data

1. Fits for CH$_2$ absorption bands

The description refers only to the 2 extreme temperatures where simultaneous fitting was done.

To calculate the tilt angle we fitted the data, obtained at 150K and 300K, using simulation procedures described in refs. 64-67. To calculate radiation propagation through the stack of Air / SAM / Si / Air we used 4×4 matrix formalism.[64] The complex dielectric function for SAM layers, $\varepsilon=\varepsilon'+i\varepsilon''$ was simulated using the Lorenz oscillator model: [66]

$$\varepsilon' = \varepsilon_\infty + \sum_i \frac{F_i(\tilde{v}_{i0}^2 - \tilde{v}^2)}{(\tilde{v}_{i0}^2 - \tilde{v}^2)^2 + (\Gamma_i\tilde{v})^2}$$

$$\varepsilon'' = \sum_i \frac{F_i\Gamma_i\tilde{v}}{(\tilde{v}_{i0}^2 - \tilde{v}^2)^2 + (\Gamma_i\tilde{v})^2} \tag{E1}$$

where F_i is the parameter for oscillator strength of the i-th oscillator, Γ_i is the full-width at half-maximum of the oscillator, and v_0 is the resonant frequency of the relevant IR mode of vibration.

To obtain initial values for the parameters F_i and Γ_i, the well-studied octadecyltrichlorosilane (OTS) layer on Si was used. The details for the fits can be found in ref. 65. When inserting the values of F_i and Γ_i of $v(CH_2)$ bands of OTS into the fits of the absorption bands of the C18 molecules under discussion, tilt angles between 25° and 32° were obtained. The error is relatively high when fitting the absolute tilt angle, due to a good convergence of fits within a wide range of possible tilt angles. In all further simulations, however, we avoided the calculations of the absolute tilt angle, and, rather, fitted on the tilt angle *difference* between the molecules at 300K and 150K when fitting simultaneously on the spectra obtained at 300K and 150K temperatures.

The chain tilt was calculated based on the relations between the transitional dipole moments and the parameters for the oscillator strength, F, discussed in detail in ref. 64. The tilt angle γ_{chain} can then be calculated from the following relations with θ_s and θ_{as}, the tilt angles of the transitional dipole moments due to CH_2 stretching vibrations:

$$\cos^2\theta_s + \cos^2\theta_{as} + \cos^2\gamma_{chain} = 1 \tag{E2}$$

where the assumption that the transition dipole moments of the symmetric and the asymmetric stretching vibrations of CH_2 group are mutually orthogonal and both are perpendicular to the chain axis when an all-trans conformation exists, was utilized.

From VIS-ellipsometric measurements, we obtained SAM thickness in the range of 2 nm - 2.1 nm using high-frequency refractive index of 1.47.[32] The value for the length of the C18, $(CH_2)_{17}CH_3$, chain is 2.23 nm, not taking into account the Si-C bond length. By projecting the measured ellipsometric thickness, the average tilt angle is $20-25^o$.

In the simulations of IR data, we fixed the room-temperature tilt angle at 25°. We point out that in this way, the simulations give a good estimation of the *difference* in the tilt angle due to the sample cooling, rather than the absolute values of the tilt angles at each temperature. The definition of relevant angles is shown in plot S6 and follows the definitions given by Rosu et al.[66]
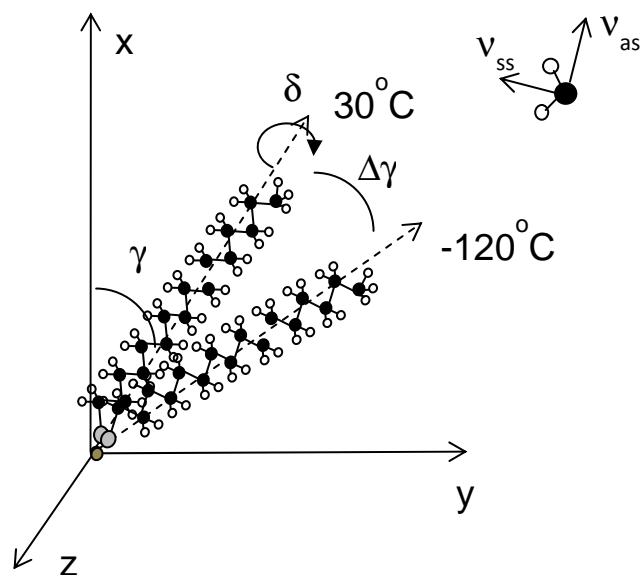
Figure S6. *Schematic model for SAM molecules used in the simulations. The tilt angle γ at 300K was fixed at $\gamma=25°$, while the fit was performed on the value of $\Delta\gamma$ until the best fit was achieved. This procedure allowed simultaneous identical adjustment of the parameters for oscillator strength, F_i, at both temperatures. The twist angle was set at 45° and was assumed to be the same in both cases.*

During the fit, the F (oscillator strength) parameters were kept identical both for 300K and 150K data. The necessary relations between the tilt angles of the principle dipole moment of the methylene vibrations and the tilt angle of the molecular chain, as well as the relevant relations connecting between the parameters for oscillator strength constants F and the tilt angles of the principle dipole moment of the methylene vibrations were used as described by Rosu et al.[66]

When lowering the temperature, both the frequency and the peak width are changing. The peak frequencies of the absorption bands were fixed at the observed measured parameters at each temperature and were not allowed to vary during the simulations. The parameters for oscillator width, Γ_i, were allowed to vary so that they can be adjusted individually for 150K data and for 300K data. However, the ratio $\Gamma_{150K}/\Gamma_{300K}$ (oscillator width Γ_i at 300 K and 150 K) was kept identical for both symmetric and

asymmetric stretching vibrations of methylene. The parameters for the FWHM ratio at different temperatures ($\Gamma_{LT}/\Gamma_{300K}$ where "LT" stands for "low-temperature") are shown in Fig. 4 (c) in the main text.

The requirement for the best fit was the convergence for *all four sets of measured data* simultaneously (s- and p- polarized data both at 300K and at 150K). Such requirement insured enough measured data for the required number of fitted parameters.

Fig. S7 shows the measured IR data along with the fitted one, where the fit is shown for the minimal obtained mean square error value for s- and p- polarized data at 300K and at 150K. At 74° angle of incidence, the best fit was achieved for tilt angle difference of $\Delta\gamma$=4.5° with $\Gamma_{150K}/\Gamma_{300K}$ =0.71. Table 1 lists the optical parameters, as obtained from the best fit, and used to plot the data in Fig. S7.

To compare our optical parameters to the reported values, we use the publication by Rosu et al.[66] who reported on $F_{tot}(\nu(CH_2)_{as})$=141,500 cm^{-2} with $\Gamma(\nu(CH_2)_{as})$=16 cm^{-1} and $F_{tot}(\nu(CH_2)_{ss})$=85,000 cm^{-2} with $\Gamma(\nu (CH_2))$= 17 cm^{-1} for monolayer of hexadecanethiol on GaAs. While our values are all at the same order of magnitude, the differences are nonetheless noticeable. One of the reasons is that the SAM molecules in our case are different, thus the oscillator values must not be the same. The other reason is that Rosu et al.[66] report on inhomogeneity in their grafted hexadecanethiol monolayers on GaAs, while in our case the density of the layers is such that no oxidation occurs at the Si/SAM interface even after prolonged storage of the samples in air.
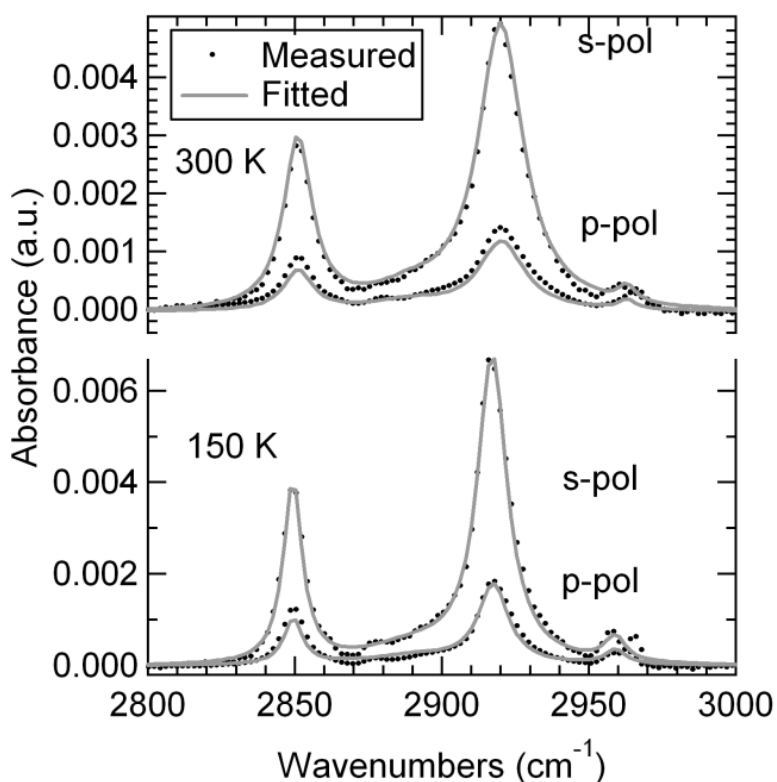
Figure S7. *Best fit obtained for simultaneous fit of four data sets, for s- and p- polarizations at 300K and at 150K, respectively. The difference in the tilt angle was $\Delta\gamma=4.5^o$ with FWHM ratio $\Gamma_{150K}/\Gamma_{300K}=0.71$. The optical parameters are shown in Table S1. Angle of incidence of IR radiation was 74° to the surface normal.*

	w_0 (300K) cm^{-1}	w_0 (150K) cm^{-1}	F_{tot} cm^{-2}	F_x cm^{-2}	Γ_{300K} cm^{-1}	$\Gamma_{150K}/\Gamma_{300K}$
$\nu(CH_2)_{as.}$	2920	2917	102000	46500	18	0.71
$\nu(CH_2)_{ss.}$	2851	2849	38500	17500	11	

Table S1. Optical parameters as fitted by the model (Eq. (E1)).

Fig. 5 in the manuscript shows the differences in the tilt angles based on the data fitted for spectra obtained in transmission at 45° angle of incidence.

Suppprting Information for SC-EDG-09-2011-000639

2. <u>Fits for CH$_3$ stretching vibrations</u>

The procedure for fitting of the CH$_3$-related absorption bands follows steps identical to those described above. We utilized an orthogonal property of the transitional dipole moments of the in-plane $\nu(CH_3)_{as}$ and out-of-plane $\nu(CH_3)_{as}$.[65] Simulations assumed all-trans conformation and C-C-C backbone angle of 109.5°. The results of the fits are presented below, from which a molecular tilt angle difference of $\Delta\gamma$=2° with error bar of 20% was calculated.
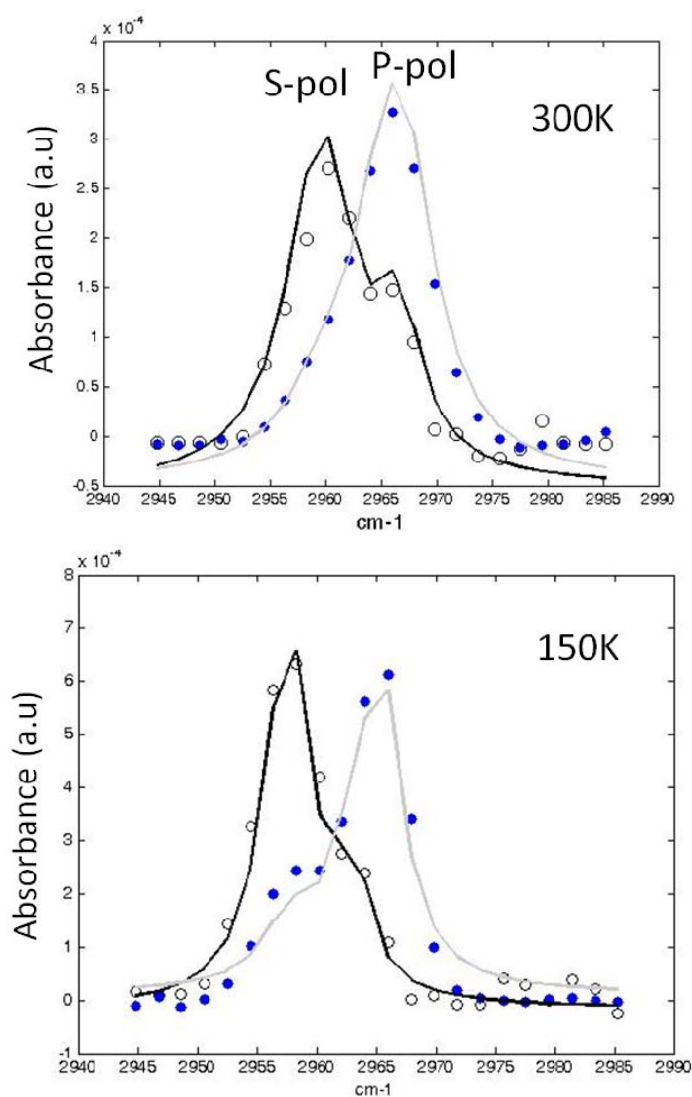
Figure S8: Fitted IR data in CH$_3$ spectral range, resulting in a molecular tilt angle difference of 2°